

Characterization, thermal and fluorescence study of Mn(II) and Pd(II) Schiff base complexes

Omyma A. M. Ali¹

Received: 16 October 2016 / Accepted: 9 December 2016 / Published online: 4 January 2017
© Akadémiai Kiadó, Budapest, Hungary 2017

Abstract 2-[(pyridin-2-ylmethylidene)amino]-6-aminopyridine (L^1), 2-[(2-furylmethylene)]phenylenediamine (L^2) and their Mn(II) and Pd(II) complexes have been synthesized as potential photoactive materials, and their structures were elucidated using a variety of physicochemical techniques. The molar conductance data reveal that all complexes are nonionic in nature. Theoretical calculations were computed using the density functional theory, where the B3LYP functional was employed. The experimental results and the calculated parameters revealed a square planar and octahedral geometry around Pd(II) and Mn(II), respectively, in which the ligands coordinate to the metal ions as a bidentate manner. The thermal decomposition of the complexes has been studied. The catalytic activity of the complexes toward hydrogen peroxide decomposition reaction was investigated at 35 and 55 °C. In addition, the synthesized ligands, in comparison with their metal complexes, were screened for their antibacterial activity.

Keywords Thermal investigation · Catalytic properties · Metal complexes · Antibacterial study

Introduction

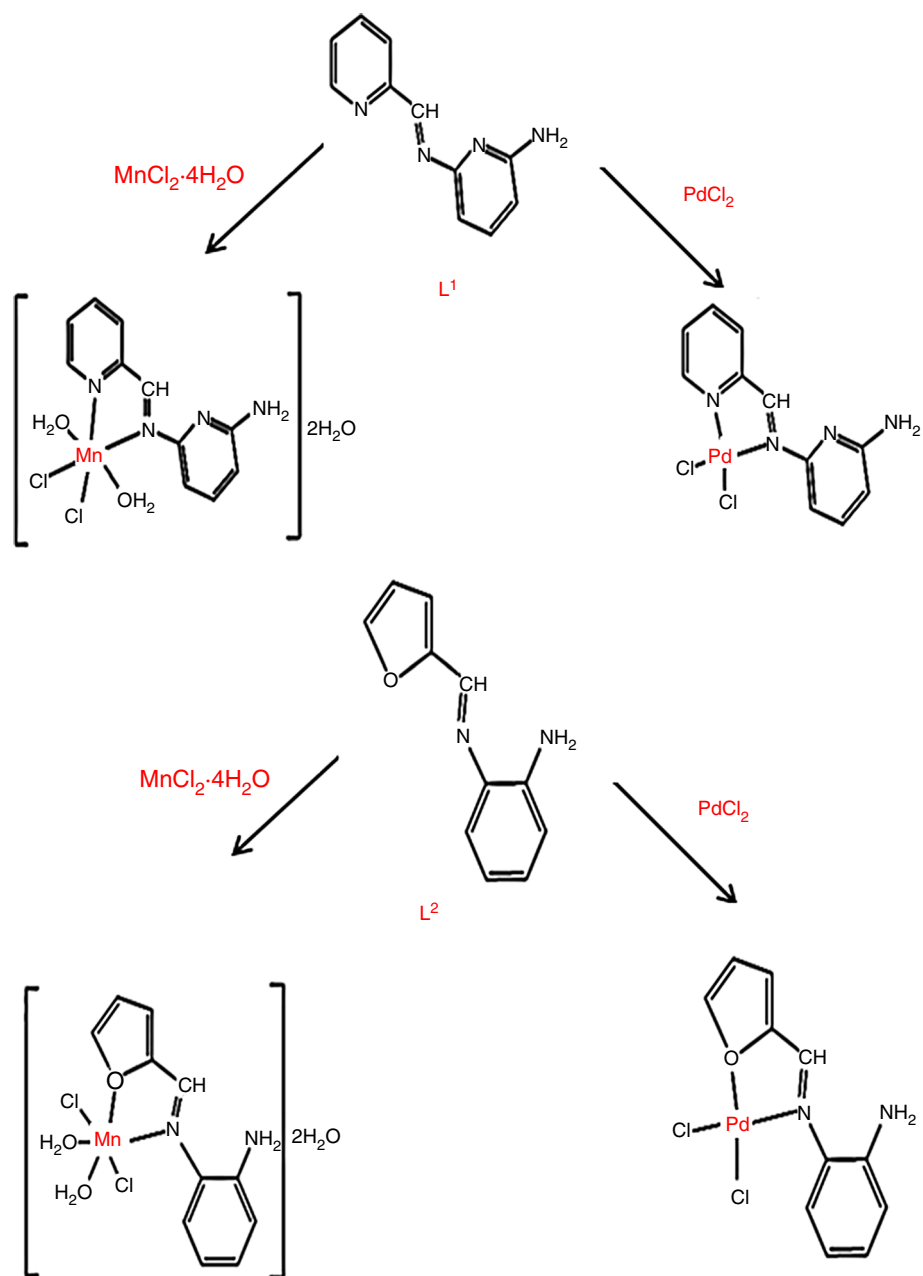
Ligands containing more than one donor sites are extensively used for the preparation of metal complexes with interesting properties. Transition metal complexes of these ligands containing pyridine, furan rings and their derivatives are also of great interest due to their ability to absorb visible light to act as electron reservoirs are promising factors in their applications as photosensitizers [1–6]. Many pyridines find application in areas where bioactivity is important, as in medicinal drugs and in agricultural products such as herbicides, insecticides, fungicides and plant growth regulators [7]. Chelating agents containing O and N donor atoms show broad biological activity [8–13] and are sensitive to the molecular environment [14, 15]. Also, Schiff base complexes show high catalytic activities in various chemical reactions such as oxidation [16, 17], epoxidation of olefins [18], homogeneous catalyst [19, 20] and polymerization of ethylene to obtain narrow molecular weight distribution [21]. Palladium complexes play an important role in bioinorganic studies in addition to their catalysis applications in many reactions [22, 23]. Schiff base complexes also have catalytic activity toward the oxidation of olefins and alcohols [24]. A lot of attention has been paid on the mono-condensed Schiff bases derived from 1,2-diamines and different aldehydes/ketones. Therefore, the present study deals with the synthesis and characterization of Mn(II) and Pd(II) complexes with mono-condensed heterocyclic Schiff base ligands, 2-[(pyridin-2-ylmethylidene)amino]-6-aminopyridine (L^1) and 2-[(2-furylmethylene)]phenylenediamine (L^2) (Fig. 1). All compounds were characterized by elemental analyses, UV–Vis, IR, ¹H-NMR spectroscopy, conductance measurements, magnetic susceptibility measurements and thermogravimetric analyses (TG). Density functional

Electronic supplementary material The online version of this article (doi:10.1007/s10973-016-6055-9) contains supplementary material, which is available to authorized users.

✉ Omyma A. M. Ali
omaymaahmed92@yahoo.com

¹ Chemistry Department, Faculty of Women for Arts, Science and Education, Ain Shams University, Cairo, Egypt

Fig. 1 Structure of ligands and their complexes



theory (DFT) calculations were done in order to correlate between the theoretical and experimental results.

Experimental

Reagents

All chemicals used were of analytical reagent grade (AR) and of the highest purity available. 2-Furancarboxaldehyde (Sigma), 2-pyridine carboxaldehyde, 2-phenylenediamine, palladium(II) chloride, manganese(II) chloride tetrahydrate and 2,6-diaminopyridine were supplied by Aldrich. The

organic solvents are reagent grade chemicals and used as received.

Instruments

Elemental analysis was performed using PerkinElmer 2400 apparatus. Infrared spectra were recorded on a Shimadzu FTIR spectrometer. ¹H-NMR spectra were run on a Bruker Avance 300 MHz instrument. UV-Vis spectra were measured on a Shimadzu UV 1800 Spectrophotometer. The photoluminescent properties were studied using a Jenway 6270 Fluorimeter. Magnetic susceptibilities were measured at room temperature using

Cambridge, England Sherwood Scientific magnetic susceptibility balance. Mass spectrometry measurements of the solid complexes (70 eV, EI) were taken on a Finnigan MAT SSQ 7000 spectrometer. Molar conductances were obtained using conductometer ORION model 150 of 0.6 Pascal's constant. Thermogravimetric analyses (TG and DTG) were carried out under N₂ atmosphere with a heating rate of 10 °C min⁻¹ using a Shimadzu DT-50 thermal analyzer.

Preparation of the ligands and their complexes

The unsymmetrical Schiff bases were synthesized according to our previously published method by monocondensation of the appropriate diamines with aldehydes [25, 26].

2-[(pyridin-2-ylmethylidene)amino]-6-aminopyridine (L¹). A solution of 2,6-diaminopyridine (0.545 g, 5 mmol) in 20 mL of ethanol was added dropwise to 2-pyridinecarboxaldehyde (0.535 g, 5 mmol) in 20 mL ethanol slowly with constant stirring. The mixture was stirred for 1 h and then refluxed for 3 h. The resulting solution was evaporated under vacuum. The precipitate was washed with ethanol and then dried in vacuum.

2-[(2-furylmethylene)]phenylenediamine (L²). A solution of O-phenylenediamine (0.541 g, 5 mmol) in 20 mL methanol was added to a methanolic solution (30 mL) of 2-furancarboxaldehyde (0.480 g, 5 mmol). A few drops of acetic acid were added to the reaction mixture and refluxed for 4 h. The mixture was concentrated by evaporation of the solvent. The product was filtered, washed with methanol and then dried in a vacuum over anhydrous calcium chloride.

Preparation of complex (1) [MnL¹Cl₂(OH₂)₂].2H₂O was prepared by the addition of a solution of L¹ (0.198 g, 1.00 mmol) in 10 mL THF to a solution of MnCl₂.4H₂O (0.198 g, 1.0 mmol) in methanol (10 mL). A mixture was left under reflux for 3 h. The product was filtered off, washed with hot petroleum ether and finally dried under vacuum.

Preparation of complex (2) [PdL¹Cl₂] was prepared by dissolving PdCl₂ (0.177 g, 1.00 mmol) in ethanol (10 mL) in the presence of a few drops of concentrated HCl. An ethanolic solution of L¹ (0.198 g, 1.00 mmol) was added dropwise to the solution of metals. The resulting mixture was allowed to reflux on a water bath for 2 h. The solid products were filtered, washing with ethanol and dried in vacuum desiccators.

Preparation of complex (3) [MnL²Cl₂(OH₂)₂].2H₂O was prepared following the same procedure as described for

[MnL¹Cl₂(OH₂)₂].2H₂O, starting with L² (0.186 g, 1.00 mmol) and MnCl₂.4H₂O (0.198 g, 1.0 mmol).

Preparation of complex (4) [PdL²Cl₂] was prepared following the same procedure as described for [PdL¹Cl₂], starting with L² (0.186 g, 1.00 mmol) and PdCl₂ (0.177 g, 1.00 mmol).

Catalytic activity studies

The metal complex (0.01 mmol) was mixed with 5 mL of H₂O₂ (0.02 M) in a flask and thermostated to 35 and 55 °C with constant stirring for 1 h. Then, the extent of undecomposed hydrogen peroxide titrating with 0.01 M KMnO₄ in the presence of 0.01 M H₂SO₄. The difference in titer values of the KMnO₄ solution before and after the catalyzed decomposition was recorded.

Antibacterial assay

The assay was carried out on the ligands and their metal complexes against two gram-positive bacteria, *B. Subtilis* and *S. aureus*, and also against two gram-negative bacteria, *E.coli* and *P. aeruginosa* microorganisms. The antibacterial susceptibility test was carried out using the agar well diffusion technique [27]. The stock solution (10 mg mL⁻¹) of the test chemical was prepared in DMSO solution. The test chemicals were added to sterile blank antimicrobial susceptibility disks. The bacteria were subcultured in agar medium. The Petri dishes were incubated for 24 h at 37 °C. The standard antibacterial drug (tetracycline) was also screened under similar conditions for comparison. Activity was determined by measuring the zones of growth inhibition surrounding the disks. Growth inhibition was compared with the standard drug. The activity results were calculated as a mean of triplicates.

DFT study

All calculations were performed with GAUSSIAN09 program package 25. The gas-phase optimized structures of the studied compounds was obtained from density functional B3LYP levels of theory using 6-31G(d) basis set for ligands and LanL2DZ basis set for complexes. The vibrational frequencies were also calculated at the same level [28].

Results and discussion

The present study is based upon the synthesized complexes of metal salts MnCl₂.4H₂O and PdCl₂ with the two Schiff bases L¹ and L². The spectroscopic and magnetic data

Table 1 Analytical and physical data of the Schiff bases and their metal complexes

Compound	C% found/calc.	H% found/calc.	N% found/calc.	m/z/P ⁺	Color/% yield	M.p./ °C	Molar conductance/ Ω ⁻¹ mol ⁻¹ cm ²
L ¹	66.45 (66.65)	5.12 (5.08)	28.75 (28.26)	198	Pale yellow (88)	250	–
(1) [MnL ¹ Cl ₂ (OH ₂) ₂].2H ₂ O	33.64 (33.35)	4.36 (4.58)	14.57 (14.14)	396	Black (80)	>300	2.3
(2) [PdL ¹ Cl ₂]	35.62 (35.18)	2.45 (2.68)	14.72 (14.92)	375	Brown (79)	>300	4.1
L ²	70.86 (70.95)	5.32 (5.41)	15.05 (15.04)	186	Brown (85)	180	–
(3) [MnL ² Cl ₂ (OH ₂) ₂].2H ₂ O	34.74 (34.40)	4.44 (4.72)	7.51 (7.29)	384	Black (88)	>300	3.1
(4) [PdL ² Cl ₂]	36.69 (36.34)	2.34 (2.77)	7.52 (7.71)	363	Brown (84)	>300	2.9

together with conductance measurements enable us to predict the possible structure of the metal complexes, which are supported also by the thermal decomposition studies. These complexes are stable in air and soluble in DMF and DMSO. The elemental analysis and physical data of the ligands and their complexes are presented in Table 1. The molar conductance values for the complexes in DMSO at a concentration of 10⁻³ M at room temperature are in the range of 2.3–4.1 Ω⁻¹ mol⁻¹ cm². The very low values indicate that these complexes behave as non-electrolytes and are neutral in nature. Mass spectrometry is an effective method for investigation of molar weight and structure of the ligands and complexes. The mass spectra of compounds exhibited a peak at a m/z value corresponding to their molecular weight (Fig. 1S).

IR spectra and mode of bonding

The IR spectra of the ligands L¹ and L² showed two bands at 3333, 3280 and 3315, 3282 cm⁻¹ due to ν_{as}(NH₂) and ν_s(-NH₂), respectively [29]. The IR spectra of the Mn(II) complexes (1) and (3) that exhibited a very strong broadband around 3336–3282 cm⁻¹ may be assigned to the stretching vibrations of ν(NH₂) group or stretching vibrations of ν(OH) of water molecules associated with the complex. In addition, the IR spectrum of L¹ displayed two bands at 1640 and 1588 cm⁻¹ due to ν(C=N) of azomethine and pyridyl moieties, respectively. The IR spectra of [MnL¹Cl₂(OH₂)₂].2H₂O (1) and [PdL¹Cl₂] (2) showed shifts in stretching vibrations of ν(C=N) for azomethine group to 1657–1627 cm⁻¹ and for pyridyl group to 1607–1591 cm⁻¹, suggesting the coordination of metal ion to azomethine and pyridyl nitrogen atoms [30]. The in-plane ring deformation band of py in free ligand L¹ (619 cm⁻¹) was shifted to higher frequencies (636–661 cm⁻¹) confirming the coordination of pyridyl nitrogen to metal [31]. The ν(C=N) stretching vibration at 1603 cm⁻¹ in the free ligand L² was shifted in the (3) and (4) complexes to 1618 and 1609 cm⁻¹, respectively, indicating the participation of azomethine nitrogen in the coordination to metal ion [32]. A medium intensity band due to ν(C–O–C) stretching vibration of furan appeared at

1240 cm⁻¹ in the ligand L² [5]. This band shifted in [MnL²Cl₂(OH₂)₂].2H₂O (3) and [PdL²Cl₂] (4) complexes to 1246 and 1290 cm⁻¹, respectively, suggesting a coordination through oxygen of furan moiety. Appearance of new bands in the spectra of complexes in the regions of 557–454 cm⁻¹ and 450–415 cm⁻¹ was assigned to ν(M–O) and ν(M–N) stretching vibration [8].

¹H NMR spectra

The ¹H NMR spectra of the free ligands L¹ and L² showed signals at 8.05 and 8.32 ppm, attributed to the azomethine (–CH=N–) protons, respectively. On complexation, the position of azomethine signal was shifted to up-field region 7.69–8.22 ppm in comparison with that of the free ligands, inferring coordination through the azomethine nitrogen atom of the ligand [33]. The ¹H NMR spectra of palladium complexes displayed a broad signal due to NH proton without shift with respect to that of the ligands confirming the non-bonding of NH₂ nitrogen to metal. In addition, the multiple signals appeared in the ¹H NMR spectra of ligands (L¹ and L²), which assigned to aromatic, pyridyl and furan protons. These multiplets were displaced upper field in the ¹H NMR spectra of Pd(II) complexes indicating the involvement of nitrogen of pyridine ring and oxygen of furan ring in the coordination. The chemical shifts of the different types of protons in the ligands and their Pd(II) complexes are listed in Table 2.

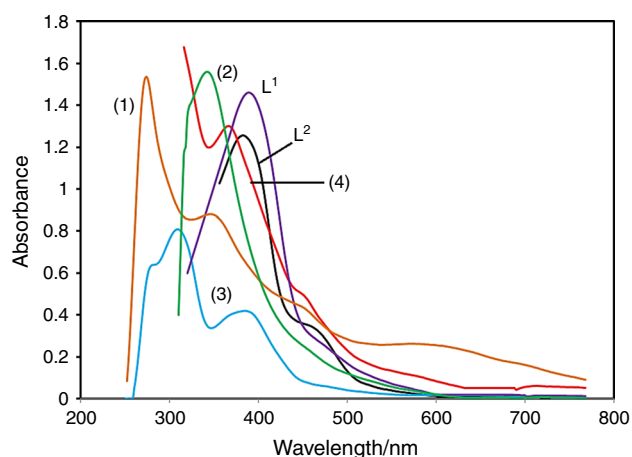
Electronic spectra and magnetic moment studies

Electronic spectra of the Schiff bases and their complexes were measured in DMSO (~1 × 10⁻⁴ M) in the range of 200–800 nm (Fig. 2). The UV–Vis absorption spectrum of the L¹ ligand in DMSO showed a strong band at 386 nm with a shoulder at 466 nm due to n–π* transitions of the non-bonding electrons present in the nitrogen of the azomethine group in the Schiff base. The electronic spectrum of the Mn(II) complex (1) consisted in four bands with the corresponding maxima at 272, 346, 448 and 590 nm due to π–π*, n–π*, ⁶A_{1g} → ⁴T_{2g} (G) and ⁶A_{1g} → ⁴T_{1g} (G), respectively [34].

Table 2 ^1H NMR spectral data of the Schiff bases and their Pd(II) complexes

Compound	Chemical shift/ δ (ppm)	Assignment
L^1	7.95–7.70 m	(7H, 4H and 3H pyridine)
	8.05 s	(1H, HC=N)
	9.99 s	(1H, NH ₂)
L^2	6.29–7.99 m	(7H, 4ArH, 3 furan H)
	8.32 s	(1H, HC=N)
	12.94 s	(1H, NH ₂)
(2) [Pd L^1 Cl ₂]	6.94–7.68 m	(7H, 4H and 3H pyridine)
	7.96 s	(1H, HC=N)
	9.99 s	(1H, NH ₂)
(4) [Pd L^2 Cl ₂]	6.45–8.04 m	(m, 8H, 4ArH, 3 furan H)
	8.22 s	(1H, HC=N)
	12.94 s	(1H, NH ₂)

s singlet, m multiplet

**Fig. 2** Electronic absorption spectra of ligands and their complexes in 10^{-4} M DMSO

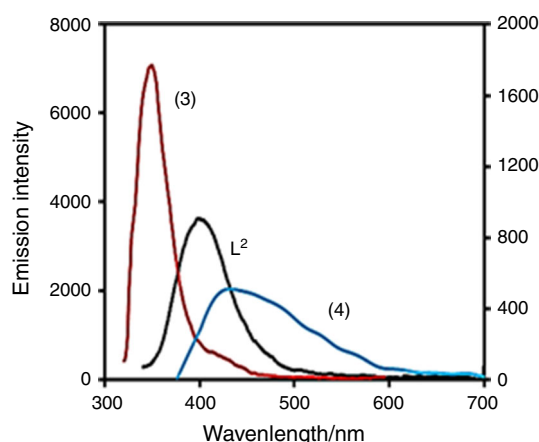
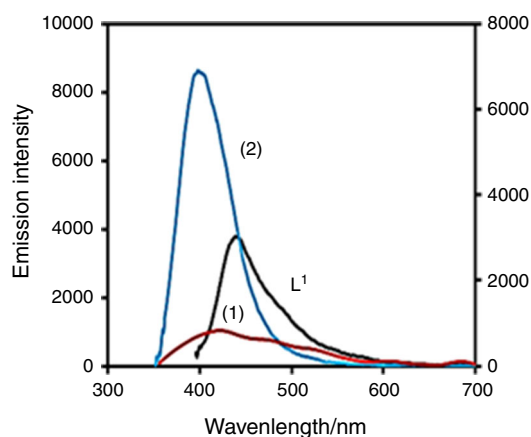
The electronic spectrum of Pd(II) complex (2) showed a band at 340 nm with a shoulder at 450 nm. These transitions may be assigned to $^1A_{1g} \rightarrow ^1E_{1g}$ and $^1A_{1g} \rightarrow ^1B_{1g}$ transitions, respectively [35]. UV-Vis spectrum of L^2 shows two bands at 380 and 458 nm due to $n-\pi^*$ transition. The electronic spectrum of the Mn(II) complex (3) showed four bands at 278, 308, 392 and 464 nm. The first two bands are due to $\pi-\pi^*$ and $n-\pi^*$ transitions, respectively. The other two bands are assigned to the transitions: $^6A_{1g} \rightarrow ^4T_{2g}$ (G) and $^6A_{1g} \rightarrow ^4T_{1g}$ (G), respectively, for a Mn(II) ion in a distorted octahedral field [36, 37]. For palladium complex 4, two absorption bands at 364 and 448 nm are observed in the spectrum due to d-d transitions [38].

The diamagnetic nature of the palladium complexes is in accordance with square planar geometry for the Pd(II) complexes [39]. The magnetic moment values for Mn(II) complexes

are in the range of 5.85–5.90 B.M. The magnetic moment lies within the region expected for octahedral complexes [40].

Fluorescence spectra studies

Fluorescence spectra of the Schiff base ligands and their complexes were measured in DMSO solution at room temperature (Fig. 3). The emission spectrum of L^1 shows band at 435 nm upon excitation at 386 nm. A broad fluorescence band centered at 417 nm observed in the emission spectrum of Mn(II) complex (1) when excited at 346 nm attributed to $\pi-\pi^*$ transitions [41]. The emission spectrum of Pd(II) complex (2) shows maxima at 394 nm on excitation at 386 nm. The fluorescence spectrum of the free L^2 when excited at 380 nm showed a maxima band at 395 nm. The emission intensity of the Mn(II) complex (3) is stronger than that of the ligand L^2 and showed a maximum at 346 nm when excited at 308 nm. Complex (4) shows very weak fluorescence at 432 nm when excited at 364 nm. Enhancement of fluorescence through complexation is, however, of much interest as it opens up the opportunity for photochemical applications of these complexes [42].

**Fig. 3** Emission spectra of ligands and their complexes in 10^{-4} M DMSO

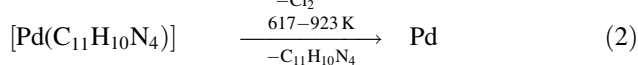
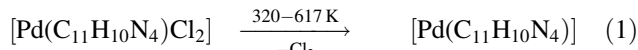
Thermal analysis (TG and DTG)

The decomposition stages, temperature ranges, decomposition product as well as mass loss percentages of the complexes are listed in Table 3.

[MnL¹Cl₂(OH₂)₂].2H₂O

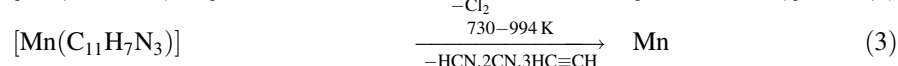
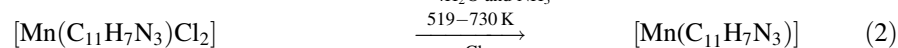
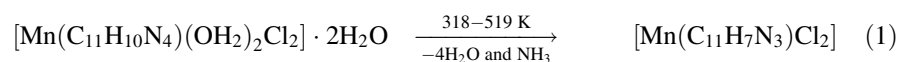
The TG curve of Mn(II) complex (1) shows the four steps of decomposition within the temperature range from 318 to 994 K (Fig. 2S). The first two decomposition stages occur in the temperature range of 318–519 K which is due to the loss of four molecules of water and NH₃ gas with an estimated mass loss of 22.50% (calcd. 22.48%). In the second decomposition step, complex (1) shows a mass loss of 17.42% (calcd. 17.89%) in the temperature range of 519–730 K, which corresponds to the removal of Cl₂ as gas. The final step of decomposition corresponds to the loss of HCN, 2CN, 3HC≡CH and 2C with the mass loss of 45.90% (calcd. 45.74%) leaving metal as a residue.

observed mass loss is 18.41%, which is consistent with the theoretical value of 18.88%. The second stage, which occurs in the temperature range of 617–923 K, corresponds to the decomposition of the organic part of ligand. The observed mass loss for this stage is 52.96% (calcd. 52.79%). The final residue was estimated as palladium metal.



[MnL²Cl₂(OH₂)₂].2H₂O

The curve of Mn(II) complex (3) was decomposed into four steps. The first two decomposition stages begin at 318 K and ends at 643 K. The observed mass loss (29.91%) is attributed to the loss of 4H₂O, NH₃ and HCN (calcd. 30.21%). The third step relates to the elimination of



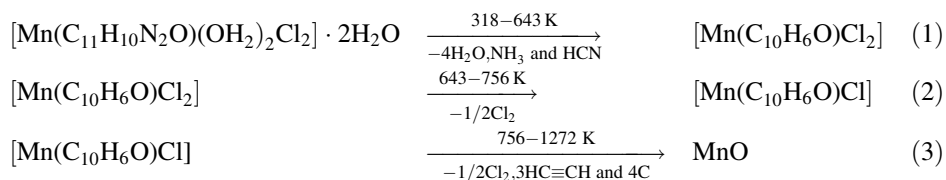
[PdL¹Cl₂]

The thermal decomposition of the Pd(II) complex (2) undergoes in two steps. The first step between 320 and 617 K corresponds to the loss of chlorine molecule. The

half chlorine in the temperature range of 643–756 K by a mass loss of 8.96% (calcd. 9.20%). The final step of the decomposition in the temperature range of 756–1272 K is due to removal of ½Cl₂, 3HC≡CH and 4C (41.71%) leaving MnO as a final residue (calcd. 42.07%).

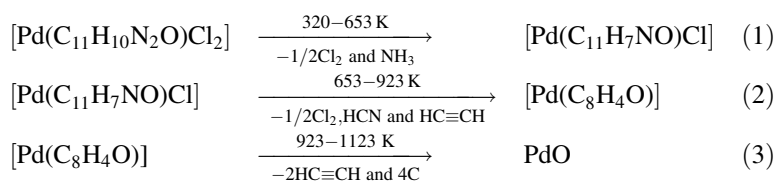
Table 3 Thermogravimetric data of complexes

Complex	TG range/K	Number of steps	Mass loss %		Assignment	Metallic residue (found)
			Calc.	Found		
(1) [MnL ¹ (OH ₂) ₂ Cl ₂].2H ₂ O	318–519	2	22.48	22.5	Loss of 4H ₂ O and NH ₃	Mn
	519–730	1	17.89	17.42	Loss of Cl ₂	(13.78%)
	730–994	1	45.74	46.3	Loss of HCN, 2CN, 3HC≡CH and 2C	
(2) [PdL ¹ Cl ₂]	320–617	1	18.88	18.41	Loss of Cl ₂	Pd
	617–923	1	52.79	52.96	Loss of L ¹	(28.63%)
(3) [MnL ² (OH ₂) ₂ Cl ₂].2H ₂ O	318–643	2	30.21	29.91	Loss of 4H ₂ O, NH ₃ and HCN	MnO
	643–756	1	9.2	8.96	Loss of ½Cl ₂	(19.42%)
	756–1272	1	42.07	41.71	Loss of ½Cl ₂ , 3HC≡CH and 4C	
(4) [PdL ² Cl ₂]	320–653	1	14.43	14.1	Loss of ½Cl ₂ and NH ₃	PdO
	653–923	1	24.34	24.73	Loss of ½Cl ₂ , HCN and HC≡CH	(33.18%)
	923–1123	1	27.52	27.99	Loss of 2HC≡CH and 4C	



[PdL²Cl₂]

The TG curve of Pd(II) complex (**4**) shows three stages of decomposition within the temperature range of 320–1123 K. The first stage of decomposition occurred in the temperature range of 320–653 K with a net mass loss of 14.10% (calcd. 14.43%), which is consistent with the elimination of ½Cl₂ and NH₃ gases (Fig. 3S). The second step involved removal of ½Cl₂, HCN and HC≡CH with a mass loss of 24.73% (calcd. 24.34%). The third step (923–1123 K) corresponds to loss of 2HC≡CH and 4C to give final PdO as a residue.



Catalytic activity studies

The decomposition of H₂O₂ catalyzed by complexes can be monitored by titrating the undecomposed H₂O₂ with a standard KMnO₄ solution. Variables such as the temperature were found to have important roles in the decomposition of H₂O₂ [43]. The Pd(II) and Mn(II) complexes were used for these investigations. The results showed that the percentage of hydrogen peroxide decomposition increased with the temperature (Fig. 4S). Pd(II) complexes are more active than Mn(II) complexes in the decomposition of hydrogen peroxide. This is due to the Pd(II) complexes have square planar structure. This provides vacant coordination sites and facilitates the formation of peroxo intermediates which are highly reactive species, leading to the rapid decomposition of hydrogen peroxide [44].

Antibacterial studies

The antibacterial studies were carried out on the ligands and their metal complexes (10 mg mL⁻¹) in DMSO solution against two gram-positive bacteria, *B. Subtilis* and *S. aureus*, and also against two gram-negative bacteria; *E.coli* and *P. aeruginosa* microorganisms. The experimental data that indicate the inhibition zone diameter (mm) of the

assayed compounds are listed in Table 1S. The results of the antibacterial activity of the compounds compared with the standard drug (Tetracycline) have indicated that compounds were active, but activity was lesser than the standard drug (Fig. 4). Comparative studies of the ligands and their metal complexes indicated that metal complexes exhibit higher antibacterial activities than the free ligands.

DFT calculations

The optimized structures of the two ligands and the corresponding four complexes are shown in Fig. 5 with the

labeling atoms. Their bond lengths and bond angles are presented in Table 4. The bond distances in (1) and (3) between manganese and both of chloro and aqua ligands are in the range (2.28–2.33 Å) and (2.01–1.96 Å), respectively. These values are in reported range [45]. The Pd–Cl,

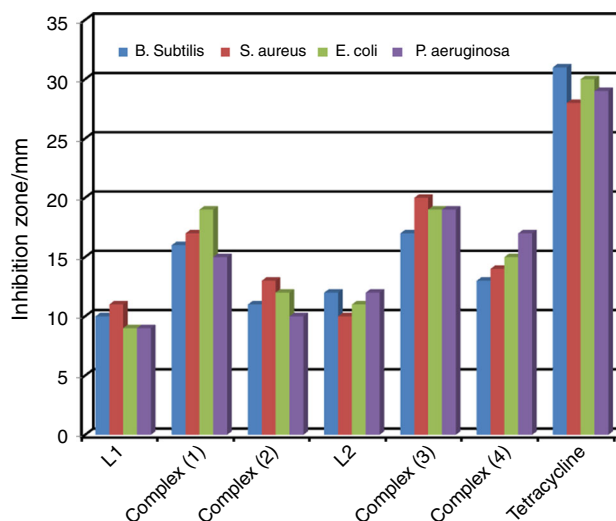


Fig. 4 Antibacterial activity of ligands and their complexes

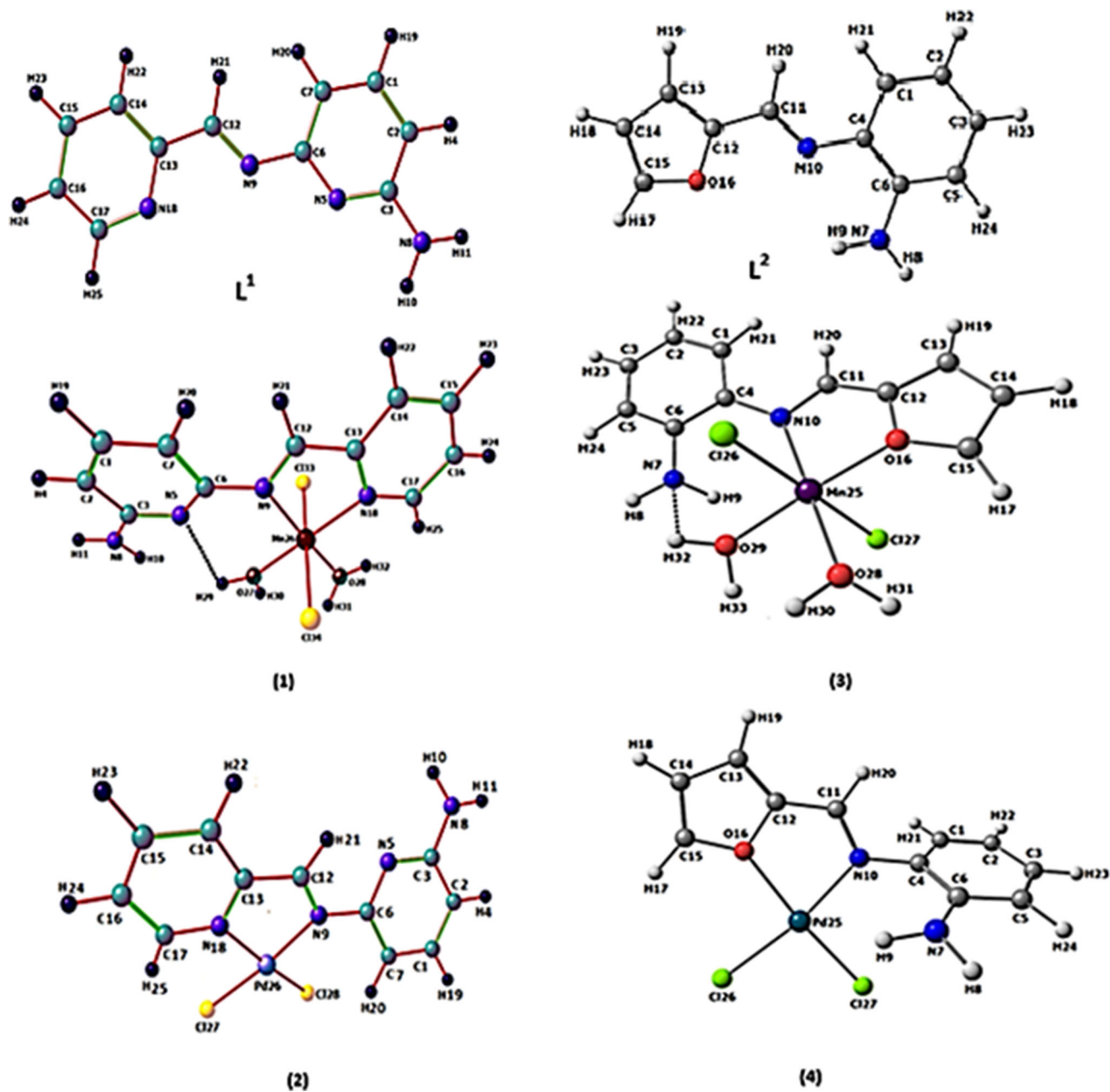


Fig. 5 Optimized geometry of the ligands and their complexes

Pd–O and Pd–N distances in complexes (2) and (4) are found to be in the reported range [46]. From the geometric parameters, Mn atoms have distorted octahedral structures, while the complexes with Pd atoms have distorted square planar structures.

Some selected calculated parameters, namely total energy and dipole moments, are available from the calculations (Table 5). The dipole moment increases spectacularly from ligands to complexes, where the electropositive metal ions induce strong polarization in the σ - and π -frameworks of the ligand molecule. In addition, the

energies of the complexes (1–4) become more negative indicating the high stability of these complexes with respect to the free ligands [46].

The calculated vibrational frequency values of the N–H, C=N, C–O–C, M–O and M–N stretching modes for the optimized complexes are tabulated in Table 6. The calculated C=N stretching frequencies for L^1 , L^2 and their Mn and Pd complexes were 1646, 1603, 1621, 1620, 1644, 1615 cm^{-1} , respectively. Corresponding experimental frequency values are 1640, 1603, 1627, 1657, 1618 and 1609 cm^{-1} , respectively. Also, the calculated stretching

Table 4 Some selected bond lengths (Å) and bond angles (°) of the optimized geometry of ligands and their complexes by using DFT/B3LYP levels of theory

Bond length/Å	L ¹	(1)	(2)	Bond length/Å	L ²	(3)	(4)
C13–N18	1.36	1.36	1.38	C12–O16	1.31	1.30	1.41
C17–N18	1.36	1.37	1.35	C15–O16	1.31	1.33	1.39
C12–N9	1.29	1.30	1.31	C11–N10	1.29	1.32	1.32
C6–N5	1.36	1.35	1.36	C4–N10	1.43	1.52	1.43
C3–N5	1.36	1.36	1.35	C6–N7	1.42	1.35	1.38
C3–N8	1.41	1.41	1.38	Mn25–O16	–	2.03	–
Mn26–N9	–	2.08	–	Mn25–O28	–	2.01	–
Mn26–N18	–	2.04	–	Mn25–O29	–	2.01	–
Mn26–O27	–	1.96	–	Mn25–Cl27	–	2.33	–
Mn26–O28	–	1.96	–	Mn25–Cl26	–	2.28	–
Mn26–Cl34	–	2.30	–	Mn25–N10	–	2.26	–
Mn26–Cl33	–	2.30	–	Pd25–N10	–	–	2.12
Pd26–N9	–	–	2.13	Pd25–O16	–	–	2.16
Pd26–N18	–	–	2.08	Pd25–Cl26	–	–	2.36
Pd26–Cl27	–	–	2.37	Pd25–Cl27	–	–	2.36
Pd26–Cl28	–	–	2.37	–	–	–	–
Bond angle/°	Bond angle/°						
C17–N18–C13	121.70	120.48	119.93	C15–O16–C12	108.89	108.15	108.45
N18–C13–C12	120.09	118.28	115.49	O16–C12–C11	124.48	120.03	114.49
C13–C12–N9	119.86	119.16	119.35	C12–C11–N10	119.56	119.33	121.12
N9–C6–N5	118.07	119.44	115.99	C4–C6–N7	120.79	119.97	121.57
N5–C3–N8	119.79	119.38	116.99	N10–Mn25–O28	–	179.81	–
N9–Mn26–O28	–	–	177.18	O16–Mn25–O29	–	176.51	–
N18–Mn26–O27	–	–	179.63	Cl26–Mn25–Cl27	–	176.83	–
Cl34–Mn26–Cl33	–	–	178.76	N10–Pd25–Cl26	–	–	169.78
N9–Pd26–Cl27	–	–	171.66	O16–Pd25–Cl27	–	–	173.63
N18–Pd26–Cl28	–	–	175.42	–	–	–	–

Table 5 Total energies (a.u.) and dipole moments (Debye) of ligands and their complexes by using DFT/B3LYP levels of theory

Parameters	L ¹	L ²	(1)	(2)	(3)	(4)
Total energy	–644.36	–610.05	–930.88	–800.84	–896.48	–766.52
Dipole moment	2.8300	1.8260	3.0231	12.7587	4.5408	10.9225

frequency values of the N–H, C–O–C, M–O and M–N modes are close to corresponding experimental IR bands. The observed differences are most probably because the calculations were performed in the gas phase, whereas the experimental results were obtained in the solid phase.

Frontier molecular orbital energies

Frontier molecular orbitals, i.e., the highest occupied molecular orbital (HOMO) and lowest unoccupied molecular orbital (LUMO) surfaces and energies for ligands and their complexes, are given in Figs. 6 and 7. Frontier

Table 6 Selected calculated IR vibration frequencies (cm⁻¹) of the ligands and their complexes

Assignment	L ¹	1	2	L ²	3	4
ν(NH ₂) or	3379	3528	3477	3343	3415	3305
ν(OH)	3217	3222	3385	3277	3236	3291
ν(C=N)	1646	1621	1644	1602	1620	1615
	1599	1579	1603			
ν(C–O–C)	–	–	–	1245	1249	1286
δ(py)	636	630	669	–	–	–
ν(M–O)	–	569	507	–	460	528
ν(M–N)	–	430	453	–	422	451

Fig. 6 Energy-level diagram of the frontier molecular orbitals for **a** L^1 and its complexes: **b** (1) and **c** (2)

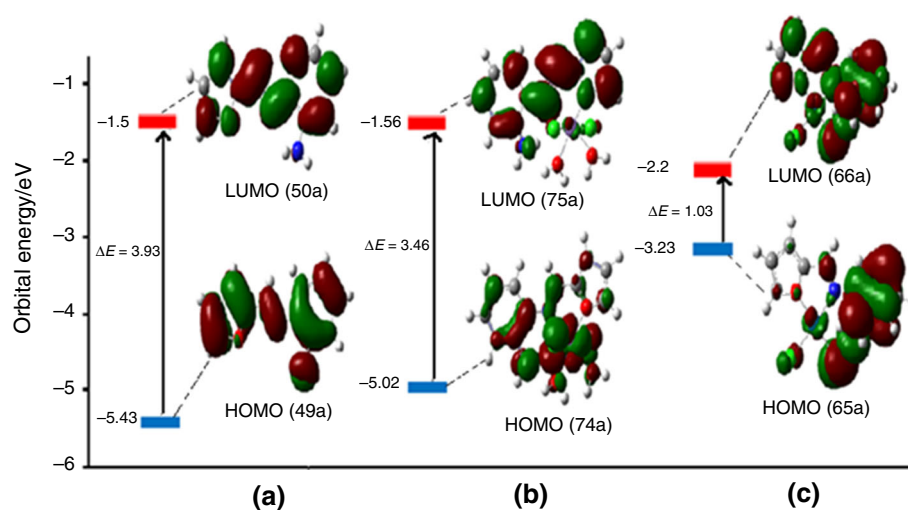
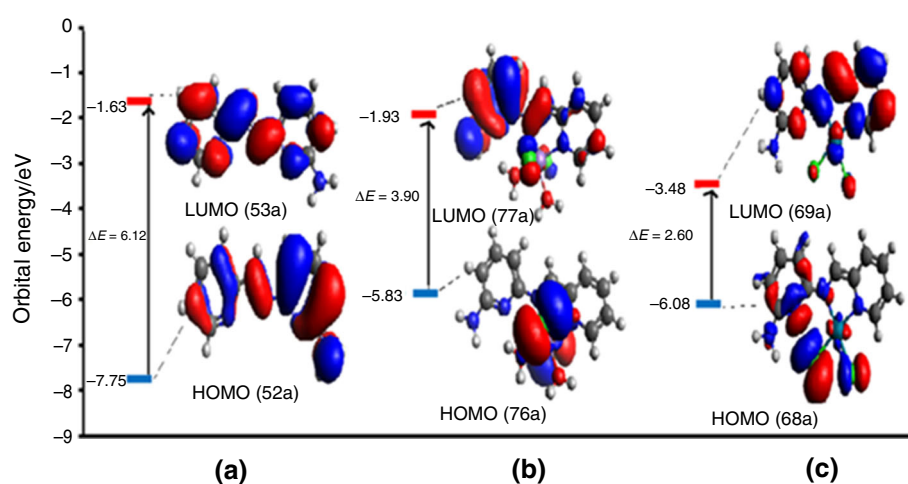


Fig. 7 Energy-level diagram of the frontier molecular orbitals for **a** L^2 and its complexes: **b** (3) and **c** (4)



molecular orbitals play an important role in the determination of chemical reactivity. HOMOs of ligands are delocalized over the whole ligand, while LUMOs electron density is not located on amino group. All LUMO of complexes is more located on azomethine, furan and pyridyl rings than HOMO of complexes. The energy of HOMO of L^1 (-7.75 eV) and L^2 (-5.43 eV) is the lowest for all compounds. The energy separation (ΔE) between the HOMO and LUMO for L^1 (1) and (2) is 3.93, 3.46 and 1.03 eV, respectively. Also, the energy gap for L^2 , (3) and (4) is 6.12, 3.90 and 2.60 eV, respectively. An electronic system with a larger HOMO–LUMO gap should be less reactive than having a smaller gap [47, 48]. The energy gaps between HOMO and LUMO (ΔE) of ligands are greater than those for manganese and palladium complexes. Hence, Mn(II) and Pd(II) complexes have more chemical activity than ligands.

Conclusions

The novel complexes of manganese(II) and palladium(II) with the bidentate ligands 2-[(pyridin-2-ylmethylene)amino]-6-aminopyridine (L^1) and 2-[(2-furylmethylene)]phenylenediamine (L^2) were synthesized and characterized using spectroscopic methods. The results of the elemental analysis, mass spectra and thermogravimetric analysis deduced the formation of 1:1 Schiff base/metal ions complexes. The optimized geometries and IR vibrational frequencies of the ligands and their complexes were calculated by the DFT method. Experimental and calculated wavenumbers were found to be in a good agreement. The complexes are biologically active. Fluorescence studies showed that the reported compounds can potentially serve as photoactive materials.

References

1. Popescu M, Rotaru P, Bubulica M-V, Kriza A. New complexes with 2-pyridyl ketone Schiff bases: synthesis, structural analysis and thermal studies. *J Therm Anal Calorim*. 2015;120:641–52.
2. Soliman AA, Amin MA, El-Sherif AA, Ozdemir S, Varlikli C, Zafer C. Synthesis and characterization of novel series of Fe(II)-mixed ligand complexes involving 2,2'-bipyridyl ligand. *Dyes Pigments*. 2013;99:1056–64.
3. Koutsouri E, Zarkadoulas A, Makedonas C, Koumbounis C, Paraskevopoulou P, Mitsopoulou CA. Combining photosensitizers: the case of $[Cl_2Pt(bpym)Re(CO)_3Cl]$ and its dithiolate analogs. *Polyhedron*. 2013;52:234–45.
4. Komatsuzaki NO, Yanagida M, Funaki T, Kasuga K, Sayama K, Sugihara H. Near-IR dye-sensitized solar cells using a new type of ruthenium complexes having 2,6-bis(quinolin-2-yl)pyridine derivatives. *Sol Energy Mater Sol Cells*. 2011;95:310–4.
5. Shakir M, Abbasi A, Khan AU, Khan SN. Synthesis and spectroscopic studies on the Schiff base ligand derived from condensation of 2-furaldehyde and 3,3'-diaminobenzidine, L and its complexes with Co(II), Ni(II), Cu(II) and Zn(II): comparative DNA binding studies of L and its Cu(II) and Zn(II) complexes. *Spectrochim Acta, Part A*. 2011;78:29–35.
6. Ali OAM. Palladium(II) and zinc(II) complexes of neutral $[N_2O_2]$ donor Schiff bases derived from furfuraldehyde: synthesis, characterization, fluorescence and corrosion inhibitors of ligands. *Spectrochim Acta, Part A*. 2014;132:52–60.
7. Gwaram NS, Ali HM, Saharin SM, Abdulla MA, Hassandarvish P, Lin TK, Ching CL, Ooi CL. Synthesis, characterization, and biological applications of some 2-acetylpyridine and acetophenone derivatives. *J Appl Pharm Sci*. 2012;2:027–38.
8. Zayed EM, Mohamed GG, Hindy AMM. Transition metal complexes of novel Schiff bases synthesis, spectroscopic characterization, and in vitro antimicrobial activity of complexes. *J Therm Anal Calorim*. 2015;120:893–903.
9. Kalinowska M, Swiderski G, Matejczyk M, Lewandowski W. Spectroscopic, thermogravimetric and biological studies of Na(I), Ni(II) and Zn(II) complexes of quercetin. *J Therm Anal Calorim*. 2016;126:141–8.
10. Ejidike IP, Ajibade PA. Synthesis, characterization and biological studies of metal(II) complexes of (3E)-3-[(2-{(E)-[1-(2,4-dihydroxyphenyl) ethylidene]amino}ethyl)imino]-1-phenylbutan-1-one Schiff base. *Molecules*. 2015;20:9788–802.
11. Sherif OE, Abdel-Kader NS. Spectroscopic and biological activities studies of bivalent transition metal complexes of Schiff bases derived from condensation of 1,4-phenylenediamine and benzopyrone derivatives. *Spectrochim Acta, Part A*. 2014;117:519–26.
12. Hanif M, Chohan ZH. Design, spectral characterization and biological studies of transition metal(II) complexes with triazole Schiff bases. *Spectrochim Acta, Part A*. 2013;104:468–76.
13. Calu L, Badea M, Chifiriuc MC, Bleotu C, David G-I, Ionita G, Marutescu L, Lazar V, Stanica N, Soponaru I, Marinescu D, Olar R. Synthesis, spectral, thermal, magnetic and biological characterization of Co(II), Ni(II), Cu(II) and Zn(II) complexes with a Schiff base bearing a 1,2,4-triazole pharmacophore. *J Therm Anal Calorim*. 2015;120:375–86.
14. Kaya I, Yildirim M, Avci A. Synthesis and characterization of fluorescent polyphenol species derived from methyl substituted aminopyridine based Schiff bases: the effect of substituent position on optical, electrical, electrochemical, and fluorescence properties. *Synth Met*. 2010;160:911–20.
15. Maxim C, Pasatou TD, Kravtsov VC, Shova S, Muryn CA, Winpenny REP, Tuna F, Andruh M. Copper(II) and zinc(II) complexes with Schiff-base ligands derived from salicylaldehyde and 3-methoxysalicylaldehyde: synthesis, crystal structures, magnetic and luminescence properties. *Inorg Chim Acta*. 2008;361:3903–11.
16. Bal S, Orhan B, Connolly JD, Digrak M, Koytepe S. Synthesis and characterization of some Schiff bases, their metal complexes and thermal, antimicrobial and catalytic features. *J Therm Anal Calorim*. 2015;121:909–17.
17. Elsherbiny AS, El-Ghamry HA. Synthesis, characterization, and catalytic activity of new Cu (II) Complexes of Schiff Base: effective catalysts for decolorization of acid red 37 dye solution. *Int J Chem Kinet*. 2015;47:162–73.
18. Kotov SV, Kolev TM, Georgieva MG. Preparation and use of novel molybdenum-containing organic complexes as catalysts in the epoxidation of cyclohexene. *J Mol Catal A: Chem*. 2003;195:83–94.
19. Das P, Linert W. Schiff base-derived homogeneous and heterogeneous palladium catalysts for the Suzuki-Miyaura reaction. *Coord Chem Rev*. 2016;311:1–23.
20. Yimer AM. Review on preparation and description of some first series divalent transition metal complexes with novel Schiff's base ligands. *Rev Catal*. 2015;2:14–25.
21. Sutar AK, Maharana T, Dutta S, Chen CT, Lin CC. Ring-opening polymerization by lithium catalysts: an overview. *Chem Soc Rev*. 2010;39:1724–46.
22. Tercero JM, Matilla A, Sanjuan MA, Moreno CF, Martin JD, Walmsley JA. Synthesis, characterization, solution equilibria and DNA binding of some mixed-ligand palladium(II) complexes. Thermodynamic models for carboplatin drug and analogous compounds. *Inorg Chim Acta*. 2003;342:77–87.
23. Ibrahim WNW, Shamsuddin M. Symmetrical palladium (II) N,N,O,O-Schiff base complex: efficient catalyst for Heck and Suzuki reactions. *Cryst Struct Theory Appl*. 2012;1:25–9.
24. Priyarega S, Tamizh MM, Karvembu R, Prabhakaran R, Natarajan K. Synthesis, spectroscopic characterization and catalytic oxidation properties of ONO/ONS donor Schiff base ruthenium(III) complexes containing $PPh_3/AsPh_3$. *J Chem Sci*. 2011;123:319–25.
25. Ali OAM, El-Medani SM, Abu Serea MR, Sayed ASS. Unsymmetrical Schiff base (ON) ligand on complexation with some transition metal ions: synthesis, spectral characterization, antibacterial, fluorescence and thermal studies. *Spectrochim Acta, Part A*. 2015;136:651–60.
26. Ali OAM, El-Medani SM, Ahmed DA, Nassar DA. Synthesis, characterization, fluorescence and catalytic activity of some new complexes of unsymmetrical Schiff base of 2-pyridinecarboxaldehyde with 2,6-diaminopyridine. *Spectrochim Acta, Part A*. 2015;144:99–106.
27. Manoharan A, Pai R, Shankar V, Thomas K, Lalitha MK. Comparison of disc diffusion and E test methods with agar dilution for antimicrobial susceptibility testing of Haemophilus influenza. *Indian J Med Res*. 2003;117:81–7.
28. Akbari A, Sheikhsaei I, Saghtforush L, Ebrahimipour SY, Amiri Z. New platinum(II) complex containing asymmetric tetra dentate Schiff base ligand synthesis, characterization and DFT calculation. *E J Chem*. 2012;9(4):2114–8.
29. Sain S, Saha R, Mostafa G, Fleck M, Bandyopadhyay D. Synthesis and crystal structure of three new copper(II) complexes with a tridentate amine and its Schiff bases. *Polyhedron*. 2012;31:82–8.
30. Khalaji AD, Das D. Thermal stability of copper(II) and nickel(II) Schiff base complexes: new precursors for preparation copper and nickel oxide nanoparticles. *J Therm Anal Calorim*. 2015;120:1529–34.
31. Booyens IN, Hlela T, Akerman MP, Xulu B. Mono- and polynuclear vanadium(IV) and -(V) compounds with 2-substituted phenylpyridyl heterocyclic chelates. *Polyhedron*. 2015;85:144–50.
32. Suresh MS, Prakash V. Preparation characterization and antibacterial studies of chelates of Schiff base derived from 4-aminoantipyrine, furfural and o-phenylenediamine. *E J Chem*. 2011;8:1408–16.

33. Mohamed GG, Omar MM, Hindy AMM. Synthesis, characterization and biological activity of some transition metals with Schiff base derived from 2-thiophene carboxaldehyde and aminobenzoic acid. *Spectrochim Acta, Part A*. 2005;62:1140–50.
34. Al-Shaalan NH. Synthesis, characterization and biological activities of Cu(II), Co(II), Mn(II), Fe(II), and UO₂(VI) complexes with a new Schiff base hydrazone: O-hydroxyacetophenone-7-chloro-4-quinoline hydrazone. *Molecules*. 2011;16:8629–45.
35. Taha ZA, Ajlouni AM, Al-Hassan KA, Hijazi AK, Faiq AB. Syntheses, characterization, biological activity and fluorescence properties of bis-(salicylaldehyde)-1,3-propylenediimine Schiff base ligand and its lanthanide complexes. *Spectrochim Acta, Part A*. 2011;81:317–23.
36. Geeta B, Shrivankumar K, Reddy PM, Ravikrishna E, Saranganpani M, Krishna Reddy K, Ravinder V. Binuclear cobalt(II), nickel(II), copper(II) and palladium(II) complexes of a new Schiff-base as ligand: synthesis, structural characterization, and antibacterial activity. *Spectrochim Acta, Part A*. 2010;77:911–5.
37. Sen S, Mitra S, Luneau D, El Fallah MS, Ribas J. Synthesis, crystal structure and magnetic properties of two new manganese Schiff base complexes [Mn₂(L¹)₂(NCS)₂] and [Mn(L²)(N₃)(H₂O)] [{L¹H=C₁₃H₁₀N₂O₂}; {L²H₂=C₁₉H₂₂N₂O₄}]. *Polyhedron*. 2006;25:2737–44.
38. Kumari N, Yadav VK, Zalis S, Mishra L. Pd(II) catalyzed transformation of Schiff bases in complexes of the type trans-[PdCl₂(NH₂Ar-X)₂] (X=H, CH₃, Cl): reactivity with aldehydes and Heck coupling reaction. *Indian J Chem*. 2012;51A:554–63.
39. Sultan JS, Lateaf SM, Rashid DK. Synthesis, characterization and antibacterial activity of mixed ligand (HL) complexes Mn(II), Co(II), Ni(II), Zn(II), Cd(II) and Hg(II) with Azide (N₃⁻). *Open J Inorg Chem*. 2015;5:102–11.
40. Tyagi M, Chandra S. Synthesis, characterization and biocidal properties of platinum metal complexes derived from 2,6-diacetylpyridine (bis thiosemicarbazone). *Open J Inorg Chem*. 2012;2:41–8.
41. Guha A, Das D. Epoxidation of olefins catalyzed by manganese(II) complexes of Schiff base ligand having N₂O coordination sphere. *Indian J Chem (A)*. 2011;50:1574–8.
42. Ali OAM, El-Medani SM, Ahmed DA, Nassar DA. Metal carbonyl complexes with Schiff bases derived from 2-pyridinecarboxaldehyde: syntheses, spectral, catalytic activity and antimicrobial activity studies. *J Mol Struct*. 2014;1074:713–22.
43. Jose J, John M, Gigimol MG, Mathew B. Synthesis, characterization, and catalytic activity of crosslinked poly(N-vinyl-2-pyrrolidone acrylic acid) copolymer–metal complexes. *J Appl Polym Sci*. 2003;90:895–904.
44. Hosny NM. Synthesis, characterization, theoretical calculations and catalase-like activity of mixed ligand complexes derived from alanine and 2-acetylpyridine. *Transition Met Chem*. 2007;32:117–24.
45. Pouralimardan O, Chamayou AC, Janiak C, Monfared HH. Hydrazone Schiff base-manganese(II) complexes: synthesis, crystal structure and catalytic reactivity. *Inorg Chim Acta*. 2007;360:1599–608.
46. Abdel Ghani NT, Mansour AM. Palladium(II) and platinum(II) complexes containing benzimidazole ligands: molecular structures, vibrational frequencies and cytotoxicity. *J Mol Struct*. 2011;991:108–26.
47. Sheikhshoaie I, Saheb V, Iranmanesh P. Some quantum chemical study on the structural properties of three unsymmetrical Schiff base ligands. *Bull Chem Soc Ethiop*. 2014;28:265–70.
48. Shah RK, Abou-Melha KS, Saad FA, Yousef T, Al-Hazmi GAA, Elghalban MG, Khedr AM, El-Metwaly N. Elaborated studies on nano-sized homo-binuclear Mn(II), Fe(III), Co(II), Ni(II), and Cu(II) complexes derived from N₂O₂ Schiff base, thermal, molecular modeling, drug-likeness, and spectral. *J Therm Anal Calorim*. 2016;123:731–43.